bacterial artificial chromosome library (ResGen, Huntsville, AL) and used as homologous fragments. The final construct is shown in Figure 2A.

The targeting vector was linearized at a unique *Asc*I restriction enzyme recognition site at the 5′-end of the long arm, and electroporated into TT2 ES cells as described previously (Murata et al., 2004; Yamanaka et al., 2008). G418-resistant clones were selected and screened by PCR with primers covering Neo (forward) and the 3′ flanking sequence of mouse *ttyh1* (reverse). The DNA sequence recognized by the reverse primer was not included in the vector. Therefore, only a 5.0-kb fragment could be PCR amplified from the DNA of the targeted ES cells using the following primer pair set: Neo (5′-ACC CGT GAT ATT GCT GAA GAG CTT GG -3′)/ Ttyh-1 (5′-TCT GAA CTA AGC CGC AGA TGT GG -3′). Of the 576 clones screened, six were positive. PCR-positive ES cell clones were also screened by Southern blotting.

*Hin*dIII-digested DNA was hybridized with a 5′ external probe that detects fragments of 12.4 kb (mutant allele) and 10.8 kb (wild-type allele) in targeted ES cells (+/−), but only a 10.8-kb fragment in wild-type cells (+/+) (left panel in Fig. 6B). *Bgl*II-digested DNA was hybridized with a 3′ external probe that detects fragments of 8.5 kb (mutant allele) and 10.0 kb (wild-type allele) in targeted ES cells (+/−), but only a 10.0-kb fragment in wild-type cells (+/+) (right panel in Fig. 6B). Clones showing homologous recombination were screened further with a Neo probe to ensure that the recombination event was unique (data not shown). Screening yielded positive ES cell clones, which were microinjected into CD-1:ICR (Charles River Japan, Yokohama, Japan). Chimeric mice were generated with two independent homologous recombinant clones.

Four male chimeras (agouti) were crossed with C57BL/6J females to generate heterozygous *ttyh1*$^{+/-}$ mice (accession no. CDB0465K; http://www.cdb.riken.jp/arg/mutant%20mice%20list.html). Germline transmission resulted in heterozygous F1 *ttyh1*$^{+/-}$ mice, confirmed by Southern blotting, that were 50% C57BL/6J in a Mendelian manner. For the current study, we used heterozygous *ttyh1*$^{+/-}$ mice, generated by crossing homozygous *ttyh1*$^{+/-}$ mice and wild-type C57BL/6J mice. Mutant animals were propagated as heterozygous colonies in a barrier facility at 23°C on a 12-hr light/dark cycle, while being backcrossed for five generations into a C57BL/6J background before generating homozygous animals by heterozygous crossings. The Institutional Animal Care and Use Committee approved the use of animals for these studies.

A three-primer PCR strategy was performed for tail genotyping, using two primers in the wild-type (wt) locus flanking the mutant cassette and one in the mutant cassette (PGK-Neo): wt forward (5′-AGG TGG CTG GCC TAT GTC CT-3′); wt reverse (5′-GAA CTG TGC ACT AAG AGC ATA-3′); and pgk reverse (5′-TAA AGC GCA TGC TCC AGA CT-3′). The wt forward plus wt reverse amplified a 361-bp band from the wild-type allele, and wt forward plus pgk reverse amplified a 250-bp band from the mutant allele. The genotype of E3.5 embryos was determined by nested PCR using wt forward and wt reverse followed by wt forward 2 (5′-TGG TTT GTC TCT TCA CCC TC-3′) and wt reverse 2 (5′-GGT CCT ATG TGC CTG TAC AT-3′) for the wild-type allele (300-bp), and wt forward and pgk reverse 2 (5′-CCA CTT GTG TAG CGC CAA GT-3′) followed by wt forward 2 and pgk reverse for the mutant allele (210-bp).

For Southern blotting, 1 cm of tails cut from the tip of offspring of heterozygous mating were incubated at 37°C for 1 hr with 75 μl of 10 mg/ml proteinase K in 675 μl of lysis buffer (10 mM Tris, pH 8.0, 10 mM EDTA, 150 mM NaCl, and 0.5% SDS). Five microliters of 10 mg/ml RNase A were added to the digested tails and incubated at 37°C for 4 hr. Digested tails were subjected to phenol/chloroform extraction and isopropanol precipitation. The pellet DNA was washed twice with 1 ml of 70% ethanol, and was air-dried before incubating in 200 μl of 10 mM Tris, pH 8, and 1 mM ethylenediaminetetraacetic acid (EDTA) overnight at 4°C.

Ten micrograms of the purified genomic DNA were digested overnight at 37°C with *Hin*dIII for the 5′ external probe, and *Bgl*II for the 3′ external and Neo probes. Digested DNA was separated on a 0.6% agarose gel, denatured with 0.5 M NaOH and 1.5 M NaCl for 45 min, and transferred to Hybond N+ filters (GE Healthcare) overnight. The membrane was then neutralized with 5× saline-sodium phosphate-EDTA (SSPE) buffer for 5 min, ultraviolet (UV) cross-linked in GS GeneLinker (Bio-Rad Laboratories), and prehybridized at 42°C for 2 hr in 50 ml of prehybridization solution (25 ml of formamide, 12.5 ml of 5× SSPE buffer, 5 ml of Denhardt's solution, 0.5 ml of 10% SDS, and 1.25 ml of 10 mg/ml sheared salmon testes DNA) and hybridized at 42°C for 16 hr with 10^6 cpm labeled probe in hybridization solution (25 ml of formamide, 12.5 ml of 5× SSPE buffer, 1 ml of Denhardt's solution, 0.5 ml of 10% SDS, 10 ml of 50% sodium dextran sulfate, and 0.5 ml of 10 mg/ml sheared salmon testes DNA). The membrane was then washed twice at room temperature (RT) for 15 min with 2× SSPE buffer containing 0.1% SDS and washed twice at 55°C for 15 min with 0.1× SSPE buffer containing 0.1% SDS before exposure to Eastman Kodak BioMax MS film (Rochester, NY) and an intensifying screen at −80°C overnight.

Radioactive probes were prepared by labeling a gel-purified PCR fragment using the Megaprime DNA labeling kit (GE Healthcare) and 32P-dCTP following the manufacturer's instructions. Free nucleotides were removed using NICK columns (GE Healthcare). The 5′ external probe was a 705-bp fragment isolated by PCR with the following primer pair: forward (5′-CAC ACA GTT GCA TTC CTG GG-3′); and reverse (5′-AAA CGG CCA CAC TTT CAG GC-3′). The 3′ external probe was a 409-bp fragment isolated by PCR with the following primer pair: forward (5′-TCT GGG TTA CGC TAT GGC G-3′); and reverse (5′-GCA GCC AAC TTG GGA TCT CCC G-3′). The Neo probe was a 650-bp fragment from the *Pst*I-*Bam*HI fragment in pKJ2-Neo.

Histochemistry

Mice were deeply anesthetized with diethylether and perfused transcardially with PBS followed by ice-cold PBS containing 4% paraformaldehyde

(PFA). The deciduas and adult mouse cerebellum were rapidly removed, post-fixed overnight at 4°C, cryoprotected in 10, 15, 20, and 30% (w/v) sucrose in 0.1 M phosphate buffer (PB) for 2 hr each at 4°C, and finally embedded in O.C.T. compound (Tissue-Tek; Sakura Finetek, Tokyo, Japan) in nitrogen-chilled isopentane for 1 min at −65°C. Serial sections (20 μm thick) in the sagittal plane were cut with a cryostat (CM1850; Leica, Nussloch, Germany), collected on precoated slides (SuperFrost; Matsunami, Osaka, Japan), and stored at −20°C before use.

For immunohistochemistry, cryosections were blocked in PBS containing 1% normal donkey serum (NDS; Chemicon, Temecula, CA), 0.3% Triton X-100, 0.25% γ-carrageenan (Sigma-Aldrich), and 0.02% sodium azide for 1 hr at RT, and incubated overnight at 4°C in a 1:250 dilution of rabbit anti-Thyh1. Sections were washed three times in PBS for 10 min, incubated at RT for 1 hr with Cy3-conjugated goat anti-rabbit IgG (1:200, Jackson ImmunoResearch Laboratories, West Grove, PA), washed once in PBS and twice in distilled water, then coverslipped using fluorescent mounting medium (Dako, Carpinteria, CA). Controls consisted of sections to which primary antibodies had not been applied. All sections were photographed using a confocal laser scanning microscope (LSM510META; Carl Zeiss, Thornwood, NY), and digital images were processed using Adobe Photoshop (San Jose, CA).

For in situ hybridization histochemistry, cryosections were permeabilized for 10 min at 37°C with 0.5 μg/ml proteinase K in DEPC-treated PBS containing 1% Tween-20 (PBST) and washed three times for 10 min with PBST. Sections were post-fixed with 4% PFA at RT for 20 min and washed with PBST.

Digoxigenin (DIG) -labeled sense and antisense cRNA probes were generated from each mouse cDNA inserted into a pBluescript II SK plasmid (Stratagene, La Jolla, CA). Sense and antisense probes were generated at 37°C for 2 hr by in vitro transcription (DIG RNA Labeling kit; Roche Diagnostics) with T3 and T7 RNA polymerase (Promega, Madison, WI), respectively. Probe cRNA was diluted to 2 μg/ml in hybridization buffer (50% deionized formamide, 5× standard saline citrate [SSC], 1% SDS, 50 μg/ml *E. coli* tRNA, and 50 μg/ml heparin) and denatured at 80°C for 5 min before application to tissue. Sections were incubated for 24 hr at 65°C in a humid chamber and washed thoroughly (twice in 5× SSC, 50% formamide, and 1% SDS and three times in 2× SSC and 50% formamide for 30 min each at 65°C, then twice with 0.05 M TBST). Sections were blocked with a 0.5% blocking reagent (Roche Diagnostics) in TBST for 1 hr at RT and incubated overnight at 4°C with alkaline phosphatase-labeled Fab fragments of sheep antibodies to DIG (1:4,000; Roche Diagnostics) in blocking solution. The sections were washed three times for 20 min in TBST, equilibrated in NTMT buffer (100 mM NaCl, 50 mM $MgCl_2$, 0.1% Tween-20, 0.1 M Tris, pH 9.5), and then developed for 2–5 days in the dark with chromogen solution in a total volume of 100 ml, containing 28 μl of 50 mg/ml 5-bromo-4-chloro-3-indolyl-phosphate (Wako, Osaka, Japan), and 54 μl of 50 mg/ml nitro-blue-tetrazolium-chloride (Wako) dissolved in NTMT buffer. The reaction was stopped with 10 mM Tris-HCl, pH 8.0, and 1 mM EDTA. Sections were counterstained with eosin, and mounted in 80% glycerol onto glass slides.

Blastocyst Culturing and Immuofluorescence Staining

Blastocysts were collected by flushing the uteri of pregnant females from *ttyh1* heterozygous crosses with Hepes-buffered medium 2 (M2; Sigma) at 3.5 dpc. For in vitro culturing, blastocysts were individually cultured for 1 day in 96-well plates containing M2 at 37 °C in 5% CO_2. All procedures for immunofluorescence staining were described previously (Yamanaka et al., 2008). Briefly, embryos were placed on precoated slides, fixed with PBS containing 4% paraformaldehyde (PFA) for 10 min at RT, and then blocked in PBS containing 1% bovine serum albumin (BSA), 10% NDS, 0.1% Tween-20 for 1 hr at RT. Slides were incubated for 2 hr at RT in a 1:250 dilution of rabbit anti-Thyh1, washed three times in PBS for 5 min, incubated at RT for 30 min with Cy3-conjugated goat anti-rabbit IgG, washed three times in PBS for 5 min, and then coverslipped using fluorescent mounting medium. All slides were photographed using a fluorescence microscope (IX70; Olympus, Tokyo, Japan), and digital images were processed using Adobe Photoshop.

Immunoelectron Microscopy

All procedures were described previously (Tomioka et al., 2005; Kuramoto et al., 2007). Briefly, pregnant mice were deeply anesthetized with diethylether and perfused transcardially with PBS followed by ice-cold 0.1 M PB containing 4% PFA, 0.5% glutaraldehyde (GA) and 4% sucrose. The embryos were rapidly removed, post-fixed for 1 hr at 4°C in 0.1 M PB with 4% PFA and 4% sucrose, and embedded in 3% agar in 0.1 M PB. Serial sections (50 μm thick) were cut with a Vibratome (VT1200S; Leica, Nussloch, Germany), collected in 0.1 M PB, and stored at 4°C before use. Floating sections were pre-fixed with PLP fixative (0.075 M PB pH 7.3, 4% PFA, 0.01 M sodium periodate, 0.15 M lysine-HCl) for 2 hr at 4°C. After washing in PBS, sections were treated with 20% NDS and 0.05% photo-flo 600 solution (Kodak) for 30 min at RT.

For immunolabeling, sections were incubated in a 1:250 dilution of rabbit anti-Thyh1 in PBS containing 2% NDS and 0.05% photo-flo 600 solution for 14 hr at 4°C. Sections were rinsed in PBS and incubated in goat anti-rabbit IgG conjugated to 1.4 nm gold particles (Nanoprobes, Yaphank, NY) in PBS containing 2% NDS and 0.05% photo-flo 600 solution for 4 hr at 4°C. The sections were rinsed in 0.1 M PB with 0.1 M sucrose, post-fixed in 0.1 M PB with 1% GA and 0.1 M sucrose for 20 min at 4°C, and enhanced using HQ silver reagents (Nanoprobes) for 5–10 min at RT. After washing, sections were post-fixed for 1 hr in 1% osmium tetroxide, dehydrated through alcohols and propylene oxide, and embedded in Epon.

Ultrathin sections (70 nm thick) were cut serially with an ultramicrotome (Reichert Ultra-CutS, Leica AG, Vienna, Austria), mounted on mesh grids for serial sectioning studies. The sections were counterstained with

uranyl acetate and lead citrate, and final preparations were analyzed on an electron microscope (H-7650, Hitachi, Japan) connected to a CCD camera.

Protein Purification and Ca^{2+}-binding Assay

For plasmid construction, partial fragments of the human *Ttyh-1* gene were amplified from a human brain cDNA pool (Clontech, Mountain View, CA) using KOD DNA polymerase (TOYOBO, Tokyo, Japan), subcloned in frame with GST into the *Eco*RI/*Sal*I restriction site of the pGEX-6p-1 expression vector (GE Healthcare), and sequenced to verify accuracy. The plasmids pGEX-h450 and pGEX-h423 were then used to transform *E. coli* strain BL21-CodonPlus (DE3)-RIL competent cells (Merck Novagen, San Diego, CA).

A 50-ml culture on LB media with 100 μg/ml ampicillin and chloramphenicol was started by inoculating a single colony. The culture was agitated for 16 hr at 250 rpm at 37°C. For GST-h450 or GST-h423 expression, the bacteria were diluted (1:20) into LB media and further grown for 2 hr at 37 °C. Protein expression was induced with 1 mM IPTG. Cells were harvested after 24 hr of incubation at 8°C by centrifugation at 2,000 *g* for 10 min at 4°C. Pellets were washed three times with PBS, resuspended in 60 ml of PBS, sonicated six times for 5 min each using Microson on ice, and incubated for 10 min at 4°C. The suspension was centrifuged at 20,000 *g* for 10 min at 4°C.

The clear supernatant was loaded on a GSTrap FF column (GE Healthcare), which was washed with 5 ml of PBS. Proteins were eluted from the column at 4°C with 5 ml of elution buffer (50 mM Tris-HCl, pH 8.0 containing 10 mM reduced glutathione). The flow-through was collected in 0.5-ml fractions and reserved until the procedure was successfully completed.

Calcium overlays on Western blots were performed as described with modifications (Maruyama et al., 1984). Briefly, equal amounts (1 μg) of protein were subjected to electrophoresis and transferred to a nitrocellulose membrane. The membrane was washed and blocked with incubation buffer (10 mM Imidazole-HCl pH 6.8, 60 mM KCl, 0.1 mM $MgCl_2$), incubated for 1 hr at RT with 4 μM $^{45}CaCl_2$ (32.9 mCi/ml, PerkinElmer, Boston, MA) in incubation buffer, washed (three times in water for 2 min each, three times in 50% ethanol for 2 min each), then exposed to Bio-Max MS film with an intensifying screen for 12 hr at RT.

ACKNOWLEDGMENTS

We thank Ms. Keiko Okamoto-Furuta and Mr. Haruyasu Kohda of the Laboratory for Electron Microscopy, Center for Anatomical Studies, Kyoto University, for expert technical assistance with immunoelectron microscopy experiments.

REFERENCES

Abramova N, Charniga C, Goderie SK, Temple S. 2005. Stage-specific changes in gene expression in acutely isolated mouse CNS progenitor cells. Dev Biol 283:269–281.

Berridge MJ, Lipp P, Bootman MD. 2000. The versatility and universality of calcium signalling. Nat Rev Mol Cell Biol 1:11–21.

Blackshaw S, Harpavat S, Trimarchi J, Cai L, Huang H, Kuo WP, Weber G, Lee K, Fraioli RE, Cho SH, Yung R, Asch E, Ohno-Machado L, Wong WH, Cepko CL. 2004. Genomic analysis of mouse retinal development. PLoS Biol 2:E247.

Burgoyne RD, Morgan A. 1998. Calcium sensors in regulated exocytosis. Cell Calcium 24:367–376.

Campbell HD, Schimansky T, Claudianos C, Ozsarac N, Kasprzak AB, Cotsell JN, Young IG, de Couet HG, Miklos GL. 1993. The Drosophila melanogaster flightless-I gene involved in gastrulation and muscle degeneration encodes gelsolin-like and leucine-rich repeat domains and is conserved in Caenorhabditis elegans and humans. Proc Natl Acad Sci U S A 90:11386–11390.

Campbell HD, Kamei M, Claudianos C, Woollatt E, Sutherland GR, Suzuki Y, Hida M, Sugano S, Young IG. 2000. Human and mouse homologues of the Drosophila melanogaster tweety (tty) gene: a novel gene family encoding predicted transmembrane proteins. Genomics 68:89–92.

Carroll J. 2001. The initiation and regulation of Ca2+ signalling at fertilization in mammals. Semin Cell Dev Biol 12: 37–43.

Kato T, Heike T, Okawa K, Haruyama M, Shiraishi K, Yoshimoto M, Nagato M, Shibata M, Kumada T, Yamanaka Y, Hattori H, Nakahata T. 2006. A neurosphere-derived factor, cystatin C, supports differentiation of ES cells into neural stem cells. Proc Natl Acad Sci U S A 103:6019–6024.

Kawaguchi A, Ikawa T, Kasukawa T, Ueda HR, Kurimoto K, Saitou M, Matsuzaki F. 2008. Single-cell gene profiling defines differential progenitor subclasses in mammalian neurogenesis. Development 135:3113–3124.

Krebs J. 1998. The role of calcium in apoptosis. Biometals 11:375–382.

Kuramoto E, Fujiyama F, Unzai T, Nakamura K, Hioki H, Furuta T, Shigemoto R, Ferraguti F, Kaneko T. 2007. Metabotropic glutamate receptor 4-immunopositive terminals of medium-sized spiny neurons selectively form synapses with cholinergic interneurons in the rat neostriatum. J Comp Neurol 500:908–922.

Maleszka R, Hanes SD, Hackett RL, de Couet HG, Miklos GL. 1996. The Drosophila melanogaster dodo (dod) gene, conserved in humans, is functionally interchangeable with the ESS1 cell division gene of Saccharomyces cerevisiae. Proc Natl Acad Sci U S A 93: 447–451.

Maruyama K, Mikawa T, Ebashi S. 1984. Detection of calcium binding proteins by 45Ca autoradiography on nitrocellulose membrane after sodium dodecyl sulfate gel electrophoresis. J Biochem 95:511–519.

Matthews CA, Shaw JE, Hooper JA, Young IG, Crouch MF, Campbell HD. 2007. Expression and evolution of the mammalian brain gene Ttyh1. J Neurochem 100:693–707.

Morciano M, Beckhaus T, Karas M, Zimmermann H, Volknandt W. 2009. The proteome of the presynaptic active zone: from docked synaptic vesicles to adhesion molecules and maxi-channels. J Neurochem 108:662–675.

Murata T, Furushima K, Hirano M, Kiyonari H, Nakamura M, Suda Y, Aizawa S. 2004. ang is a novel gene expressed in early neuroectoderm, but its null mutant exhibits no obvious phenotype. Gene Expr Patterns 5:171–178.

Nixon VL, McDougall A, Jones KT. 2000. Ca2+ oscillations and the cell cycle at fertilisation of mammalian and ascidian eggs. Biol Cell 92:187–196.

Poenie M, Alderton J, Tsien RY, Steinhardt RA. 1985. Changes of free calcium levels with stages of the cell division cycle. Nature 315:147–149.

Rae FK, Hooper JD, Eyre HJ, Sutherland GR, Nicol DL, Clements JA. 2001. TTYH2, a human homologue of the Drosophila melanogaster gene tweety, is located on 17q24 and upregulated in renal cell carcinoma. Genomics 77:200–207.

Ratan RR, Maxfield FR, Shelanski ML. 1988. Long-lasting and rapid calcium changes during mitosis. J Cell Biol 107: 993–999.

Suzuki M, Mizuno A. 2004. A novel human Cl(-) channel family related to Drosophila flightless locus. J Biol Chem 279:22461–22468.

Toiyama Y, Mizoguchi A, Kimura K, Hiro J, Inoue Y, Tutumi T, Miki C, Kusunoki M. 2007. TTYH2, a human homologue of the Drosophila melanogaster gene tweety, is up-regulated in colon carcinoma and involved in cell proliferation and cell aggregation. World J Gastroenterol 13:2717–2721.

Tombes RM, Borisy GG. 1989. Intracellular free calcium and mitosis in mammalian cells: anaphase onset is calcium modulated, but is not triggered by a brief transient. J Cell Biol 109:627–636.

Tomioka R, Okamoto K, Furuta T, Fujiyama F, Iwasato T, Yanagawa Y, Obata K, Kaneko T, Tamamaki N. 2005. Demonstration of long-range GABAergic connections distributed throughout the mouse neocortex. Eur J Neurosci 21: 1587–1600.

Vergara C, Latorre R, Marrion NV, Adelman JP. 1998. Calcium-activated potassium channels. Curr Opin Neurobiol 8: 321–329.

Yamanaka Y, Heike T, Kumada T, Shibata M, Takaoka Y, Kitano A, Shiraishi K, Kato T, Nagato M, Okawa K, Furushima K, Nakao K, Nakamura Y, Taketo MM, Aizawa S, Nakahata T. 2008. Loss of Borealin/DasraB leads to defective cell proliferation, p53 accumulation and early embryonic lethality. Mech Dev 125:441–450.

TISSUE ENGINEERING: Part C
Volume 16, Number 1, 2010

DOI: 10.1089/ten.tec.2008.0693

A Novel Method to Isolate Mesenchymal Stem Cells from Bone Marrow in a Closed System Using a Device Made by Nonwoven Fabric

Kinya Ito, M.D.,[1,2] Tomoki Aoyama, M.D., Ph.D.,[1] Kenichi Fukiage, M.D.,[1,3] Seiji Otsuka, M.D., Ph.D.,[1,2] Moritoshi Furu, M.D.,[1,3] Yonghui Jin, M.D.,[1] Akira Nasu, M.D.,[1,3] Michiko Ueda,[1] Yasunari Kasai,[4] Eishi Ashihara, M.D., Ph.D.,[4] Shinya Kimura, M.D., Ph.D.,[4] Taira Maekawa, M.D., Ph.D.,[4] Akira Kobayashi, Ph.D.,[5] Shinya Yoshida, Ph.D.,[5] Hideo Niwa, Ph.D.,[5] Takanobu Otsuka, M.D., Ph.D.,[2] Takashi Nakamura, M.D., Ph.D.,[3] and Junya Toguchida, M.D., Ph.D.[1]

Bone marrow stromal cells (BMSCs) include cells with multidirectional differentiation potential described as mesenchymal stem cells. For clinical use, it is important to develop a way to isolate BMSCs from bone marrow in a closed system without centrifugation. After screening 200 biomaterials, we developed a device containing a nonwoven fabric filter composed of rayon and polyethylene. The filter selectively traps BMSCs among mononuclear cells in bone marrow based on affinity, not cell size. The cells are then recovered by the retrograde flow. Using canine and human bone marrow cells, the biological properties of BMSCs isolated by the device were compared with those obtained by conventional methods using centrifugation. The total number isolated by the device was larger, as was the number of $CD106^+/STRO\text{-}1^+$ double-positive cells. The cells showed osteogenic, chondrogenic, and adipogenic differentiation potential *in vitro*. Finally, the direct transplantation of cells isolated by the device without *in vitro* cultivation accelerated bone regeneration in a canine model of osteonecrosis *in vivo*. The proposed method is rapid and efficient, does not require a biological clean area, and will be useful for the clinical application of mesenchymal stem cells in bone marrow.

Introduction

Bone marrow stromal cells (BMSCs) include cells with multidirectional differentiation potential such as mesenchymal stem cells (MSCs), multipotent adult progenitor cells, and marrow-isolated adult multilineage inducible cells, although it is not yet clear whether these cell types are distinct or overlap.[1,2] In spite of such ambiguity, BMSC-derived multipotent cells have been used in various fields of regenerative medicine. For clinical applications, however, it is critical to develop a method separating BMSCs containing multipotent cells from other types of cells in bone marrow that is simple, safe, inexpensive, and achievable in a closed system. The most popular way to isolate BMSCs is the density gradient method using a detergent such as sucrose[3] although the process is technically demanding and time consuming. Simple centrifugation with low gravity can also separate mononuclear cells (MNCs) from erythrocytes, and BMSCs can be selected through adherence to plastic dishes.[4] This method, however, still needs centrifugation, which makes it difficult to perform in a closed system, and therefore requires a biologically clean room.

To avoid the need for centrifugation, we have attempted to develop a device that can isolate BMSCs by filtration, and have selected nonwoven fabrics as biomaterials. Nonwoven fabrics are engineered materials that provide specific functions such as absorbency, liquid repellency, resilience, stretch, softness, strength, flame retardancy, washability, and cushioning.[5] As for clinical applications, nonwoven fabrics are used mainly for two purposes, as scaffolds and filters. A number of studies have used nonwoven fabrics as scaffolds for tissue regeneration.[5–7] The material and diameter of the fabric are important for cell attachment.[6,8] For example, polyethylene terephthalate with fibers 9.0 μm in diameter is ideal for the osteogenic differentiation of MSCs.[6] As filters, nonwoven fabrics have been used to sterilize medical materials.[9] Lymphocytapheresis is a form of treatment for patients with autoimmune diseases, in which lymphocytes in

[1]Institute for Frontier Medical Sciences, Kyoto University, Kyoto, Japan.
[2]Department of Orthopaedic Surgery, Graduate School of Medical Sciences, Nagoya City University, Nagoya, Japan.
[3]Department of Orthopaedic Surgery, Graduate School of Medicine, Kyoto University, Kyoto, Japan.
[4]Department of Transfusion Medicine and Cell Therapy, Kyoto University Hospital, Kyoto, Japan.
[5]Kaneka Co., Osaka, Japan.

peripheral blood are removed to reduce immunoreactions. To replace the centrifugation process in lymphocytapheresis, a filtration method using nonwoven fabrics has been developed.[10] The trapping effect is attributed to the affinity of the material for cells and the size of the material's fibers, with almost all leukocytes trapped when the fibers are less than 3 μm in diameter.[10,11]

As pure mechanical trapping based on cell size can damage cell membranes, we have tried to develop a filter that traps MSCs through affinity and here show that a new device composed of rayon–polyethylene nonwoven fabrics can isolate BMSCs from bone marrow aspirates, which contain cells compatible with multipotent cells *in vitro* and *in vivo*.

Materials and Methods

Screening of materials

The basic concept behind our approach is to trap BMSCs among bone marrow aspirates on a filter, and collect them using a retrograde flow (Fig. 1A). Biomaterials for the filter were screened based on microscopic structure (evenness), diameter (over 10 μm), weight (over 50 g/m^2), bio-safety, and availability (as the first screening). Potentially suitable biomaterials were further screened by conducting colony-forming unit (CFU) assays described later using swine bone marrow cells in three steps (as the second, third, and fourth screening; Supplemental Fig. S1, available online at www.liebertonline.com).

Electron microscopic analyses

After bone marrow had permeated through it, the filter was treated with 2.5 wt% glutaraldehyde in saline for 2 days at 4°C. The samples were dried by passing them through a series of graded-alcohol-saline solutions. Finally, the solution was changed to 100% t-butanol, and the samples were freeze-dried for 10 h at −5°C. The dried membranes were coated with gold–palladium and examined using a S-3000N scanning electron microscope (Hitachi, Tokyo, Japan).

Harvesting of bone marrow

Humans. Ten milliliters of bone marrow was taken from iliac crests of donors who received orthopedic operative procedures requiring autologous bone grafts from iliac crests. The donors had no history of concurrent illness or of medication that could affect bone metabolism. The Ethics Committee of the Faculty of Medicine, Kyoto University, approved the procedure, and informed consent was obtained from each donor according to the declaration of Helsinki.

Dogs. Ten milliliters of bone marrow was aspirated from iliac crests of male beagle dogs (10–13 kg) under intravenous anesthesia. The experiments with animals were approved by the institutional animal research committee, and performed according to the Guidelines for Animal Experiments of Kyoto University.

Preparation of MNCs

Human marrow samples were divided equally into three aliquots (3 mL each). One aliquot was applied to the device (method D), which had been saturated with saline. After washing the filter with 10 mL of saline, trapped cells were collected by a retrograde flow of the culture medium into a collection bag (Fig. 1A). The second aliquot was suspended in 5 mL of α-minimum essential medium GlutaMAX (Invitrogen, Carlsbad CA,) with 10% fetal bovine serum (Hyclone, South Logan, UT). The suspension was centrifuged at 1200 rpm for 5 min. The supernatant and the buffy coat were re-suspended in another tube with 5 mL of α-minimum essential medium GlutaMAX with 10% fetal bovine serum. This method is hereafter designated method S (simple centrifugation).[4,12] The final aliquot of bone marrow was fractionated by centrifugation over a density cushion using a Ficoll gradient (GE Healthcare Life Sciences, Piscataway, NJ), as described.[3] The interface layer was harvested and washed twice with 10 mL of Hank's buffer solution. This method is hereafter designated method F (Ficoll gradient).

Collection efficacy

Cells trapped on the filter and collected by retrograde flow in the collection bag were designated the collected fraction, and cells flowing through the filter into the flow-through bag were designated the flow-through fraction (Fig. 1A). Collection efficacy was determined as the ratio of the number of cells in each fraction to that in the applied bone marrow.

CFU assay

For the CFU assay, the MNCs were diluted and plated in 60-mm cell culture dishes at a density of 2.5×10^5 cells/dish and incubated for 14 days ($n=3$). The cells were fixed with methanol and stained with a 0.05% crystal violet solution. We counted the number of colony with a diameter more than 4 mm.

Flow cytometry

Cells were stained at room temperature for 30 min with the following antibodies: CD10-phycoerythrin (PE), CD34-allophycocyanin (APC), CD45-peridinin chlorophyll protein (PerCP-Cy5.5), CD106-fluorescein isothiocyanate (FITC), CD166-PE (BD Biosciences, San Jose, CA), CD90-FITC (Beckman Coulter, Fullerton, CA), CD271-APC (Miltenyi Biotec, Bergisch Gladbach, Germany), and STRO-1-PE (Santa Cruz Biotechnology, Santa Cruz, CA). They were subsequently subjected to flow cytometry using a FACS Calibur instrument (BD Biosciences).

Induction of differentiation and histochemical evaluating

Differentiation was induced using the standard method.[13] The differentiation potential was evaluated as below.

- Osteogenic differentiation: Calcified nodules were evaluated by alizarin red staining, and calcium content was quantified.
- Adipogenic differentiation: Intracellular lipid droplets were stained with oil red-O, and the amount of triglyceride was quantified.
- Chondrogenic differentiation: Cartilage matrix was evaluated by alcian blue staining, and the amount of glycosaminoglycan was quantified.

These analyses were described previously.[14]

Reverse transcription–polymerase chain reaction

Total RNA was extracted using RNeasy Kit (Qiagen, Hilden, Germany). All reverse transcription reactions were

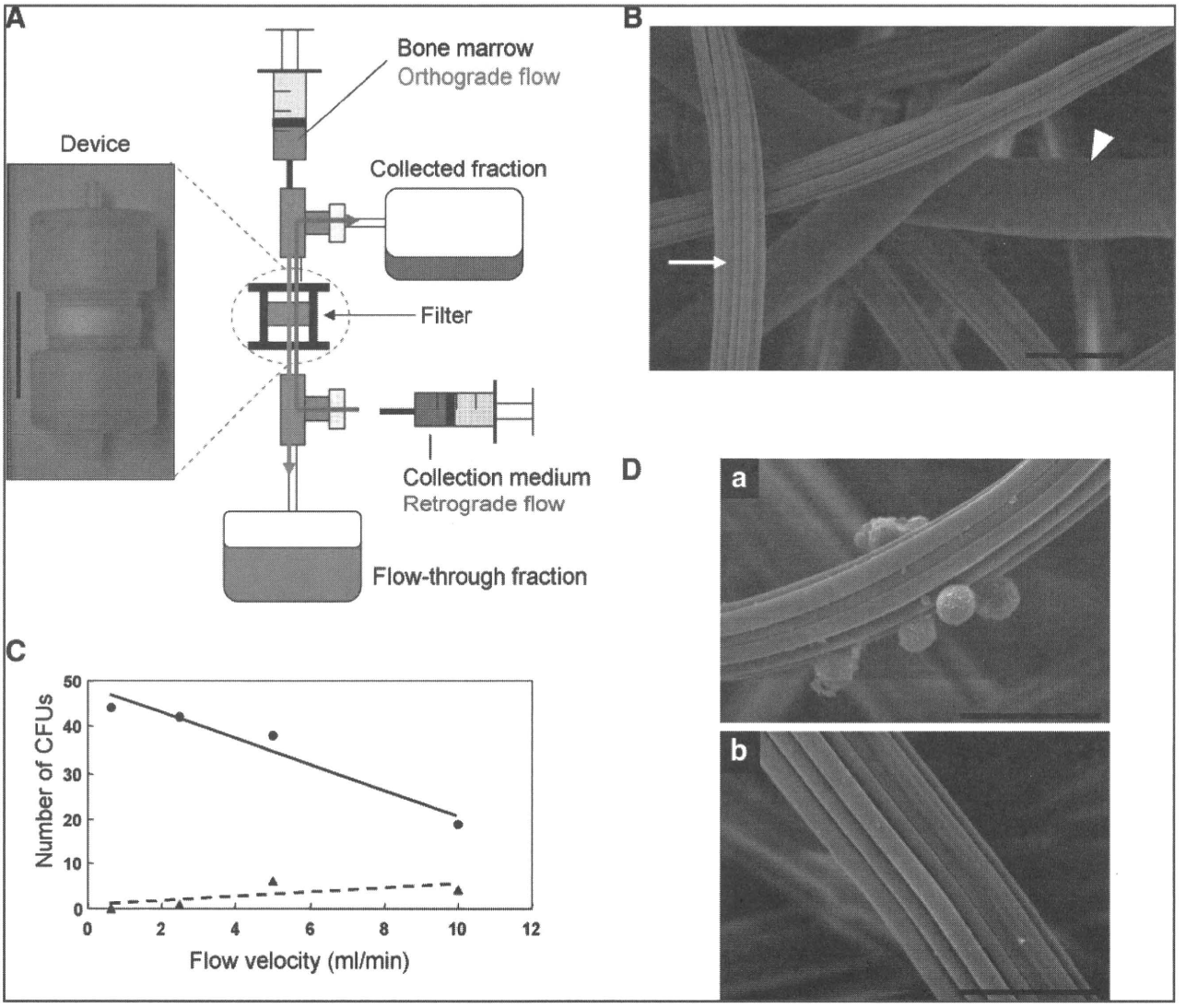

FIG. 1. Device containing a nonwoven fabric filter. (**A**) Photo of the device and schematic explanation of the collection method. The red line indicates the orthograde flow to apply bone marrow, and the blue line indicates the retrograde flow to collect cells. Scale bar = 30 mm. (**B**) Electron micrograph of the nonwoven fabric of rayon and polyethylene. Arrow, rayon; arrowhead, polyethylene. Magnification, 2000×. Scale bar = 20 μm. (**C**) Conditioning of flow velocity using swine bone marrow. Closed circles and closed triangles indicate the number of colony-forming units (CFUs) formed by cells in the collected fraction and flow-through fraction at the indicated flow velocity, respectively. (**D**) Electron micrograph of the surface of the filter after the orthograde flow of swine bone marrow (a) and after the retrograde flow of collection medium (b). Magnification, 2500×. Scale bar = 20 μm.

performed using the Super Script First Strand Synthesis System (Invitrogen). Polymerase chain reaction amplification was carried out using rTaq polymerase (Toyobo, Osaka, Japan). All polymerase chain reactions were performed using GeneAmp 9700 (PE Applied Biosystem, Foster City, CA) and specific primers for each gene.[14]

Preparation of the canine model of osteonecrosis and cell transplantation

A canine model of scapho-lunate osteonecrosis was prepared as described previously.[15] Briefly, scapho-lunates on one side were exposed dorsally, and a cortical window of 5×10 mm was made, through which as much cancerous bone as possible was removed. After the curettage, the cavity was filled with liquid nitrogen for 10 min, and the frozen bone was thawed at room temperature for 10 min. This freeze–thaw procedure was repeated three times. On one side, the bone cavity was filled with beta-tricalcium phosphate (β-TCP) granules (200 μg, 0.2 cm^3) (Osferion®; Olympus, Tokyo, Japan) (hereafter designated the control side). On the other side, canine BMSCs ($6.0\times10^7 \pm 1.5\times10^7$) isolated by the device from 10 mL of bone marrow were mixed with the same amount of β-TCP and transplanted into the bone cavity (hereafter designated the BMSC side). Finally, the bone window was plugged with 5×10 mm cortical bone. Animals were sacrificed and evaluated at 4 weeks after the operation ($n = 6$).

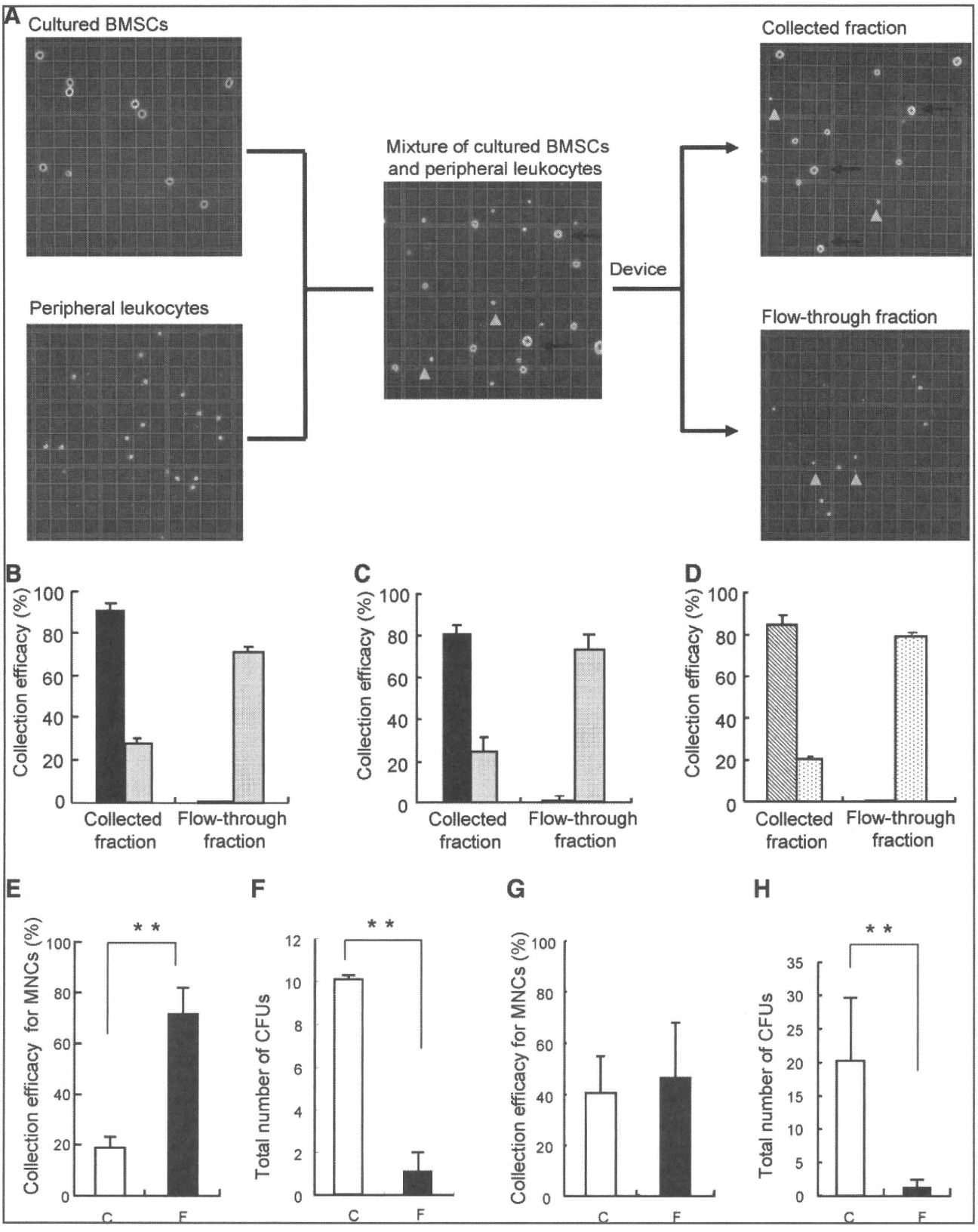
A
Cultured BMSCs
Peripheral leukocytes
Mixture of cultured BMSCs and peripheral leukocytes
Device
Collected fraction
Flow-through fraction
B
C
D
Collection efficacy (%)
Collected fraction
Flow-through fraction
E
F
G
H
Collection efficacy for MNCs (%)
Total number of CFUs
* *
C
F

Imaging analyses

X-ray. Antero-posterior and lateral views of both wrists were obtained. The carpal height ratio was calculated from the antero-posterior view.[15,16] The Ståhl index was calculated from the lateral view.[15,17]

Micro-computed tomography. Canine carpal bones were scanned by computed tomography (CT) (SMX-100CT-SV3 type; Shimazu, Kyoto, Japan). The image consisted of 800 slices with a voxel size of 68.224 mm in all three axes. Coronal and sagittal cross-sectional views of the scapho-lunate were reconstructed using adjunctive software. The same setting was used for all samples. The image reconstruction and quantification of the scapho-lunate were performed with VG Studio MAX software (Nihon Visual Science, Tokyo, Japan).[15]

Macroscopic and microscopic assessments

The volume and weight of extracted scapho-lunate bones were actually measured using a scale. The samples were fixed in a 10% formalin solution, decalcified with Plank-Rychlo solution, and then embedded in paraffin. Serial sections were cut at 4 μm, and stained with hematoxylin–eosin and silver impregnation.

Using a light microscope, the absorption of β-TCP granules and the formation of bone were graded as follows.[18] For hematoxylin–eosin staining, granules were not surrounded by cells or newly forming bone (grade 1); granules were surrounded by osteoblasts and/or osteoclasts (grade 2); and granules were surrounded by newly forming bone (grade 3). For silver impregnation staining, granules were not completely surrounded by collagen fibrils (grade 1); granules were completely surrounded by collagen fibrils (grade 2); and granules were completely eroded with reticulated collagen fibrils (grade 3). All the β-TCP granules in a whole section were classified according to the three grades. The rates of each grade were then calculated.

Statistics

Results are expressed as the mean ± SE. The statistical analysis was first performed by the analysis of variance (ANOVA), and if there was a significant difference among samples, Turkey's *post hoc* test was performed for multiple comparisons. The Student's *t*-test was carried out to compare individual data. A significant difference was accepted at $p < 0.05$.

Results

Screening of materials

The first screening, of 200 potential biomaterials for the filter, was based on the parameters described in the Materials and Methods section. Forty materials were then selected for the second screening using swine bone marrow cells ($n = 2$). Ten biomaterials showed CFU counts of more than 10, and were selected for the third screening by CFU assay ($n = 3$), of which six preceded to the fourth and last screening ($n = 3$). Finally, a rayon–polyethylene nonwoven fabric was selected as the material for the filter (Supplemental Fig. S1, available online at www.liebertonline.com). First, the optimum velocity of filtration was determined by comparing CFU counts of cells in the collected and flow-through fractions. A velocity of 2.5 mL/min was chosen for further experiments (Fig. 1C). Electron microscopic analysis confirmed the binding of swine bone marrow cells and their detachment under retrograde flow (Fig. 1D, a and b).

Selective collection of BMSCs by the device

To analyze the device's selectivity, cultured human BMSCs or peripheral leukocytes were applied to it, and the cells in the collected fraction and flow-through fractions were enumerated (Fig. 2B). More than 90% of BMSCs were collected in the collected fraction, compared to only 28% of peripheral leukocytes (Fig. 2B). This selectivity was also observed when equal numbers (1×10^6) of BMSCs and peripheral leukocytes were mixed and then applied to the device (Fig. 2C). Because BMSCs and peripheral leukocytes differ in size, we could distinguish between them in the cell counting chamber (Fig. 2A). Approximately 80% of BMSCs were collected in the collected fraction, and an almost equal percentage of peripheral leukocytes were collected in the flow-through fraction (Fig. 2C). More than 90% of $CD44^+$ cells were collected with the device, leaving almost no $CD44^+$ cells in the flow-through fraction, whereas less than 20% of $CD45^+$ cells were collected (Fig. 2D). These results suggested the selective collection of BMSCs by the device.

FIG. 2. Selective collection of bone marrow stromal cells (BMSCs) with CFUs by the device. (**A**) Selective counting of BMSCs and peripheral leukocytes. BMSCs and peripheral leukocytes differed in morphology in the cell counting chamber (left two photos). After the mixing of the two types of cells (middle) and application of the device, each type of cell in the collected (right upper) or flow-through (right lower) fraction was numerated. Arrow, cultured BMSCs; arrowhead, peripheral leukocytes. (**B**) Collection efficacy for human BMSCs (black box) and peripheral leukocytes (gray box). Each type of cell was applied to the device separately, and collection efficacy was calculated from the number of cells in the collected and flow-through fractions. (**C**) Collection efficacy for human BMSCs (black box) and peripheral leukocytes (gray box). Equal numbers of BMSCs and peripheral leukocytes were mixed and applied to the device. Collection efficacy was calculated from the number of cells in the collected and flow-through fractions. (**D**) Collection efficacy for CD44 (hatched box) and $CD45^+$ (dotted box) cells. Equal numbers of BMSCs and peripheral leukocytes were mixed and applied to the device. Cells positive for CD44 or CD45 in the collected or flow-through fraction were numerated by fluorescence-activated cell sorting (FACS), and collection efficacy was calculated from the number of positive cells in the cell mixture before the treatment. (**E**) Collection efficacy for mononuclear cells (MNCs) from canine bone marrow. $^{**}p < 0.01$ (**F**) Total number of CFUs derived from canine MNCs collected in the collected and flow-through fractions. From the results on collection efficacy and number of CFUs, the total number of CFUs was calculated. $^{**}p < 0.01$. (**G**) Collection efficacy for MNCs from human bone marrow. (**H**) Total number of CFUs derived from human MNCs collected in the collected and flow-through fractions. $^{**}p < 0.01$.

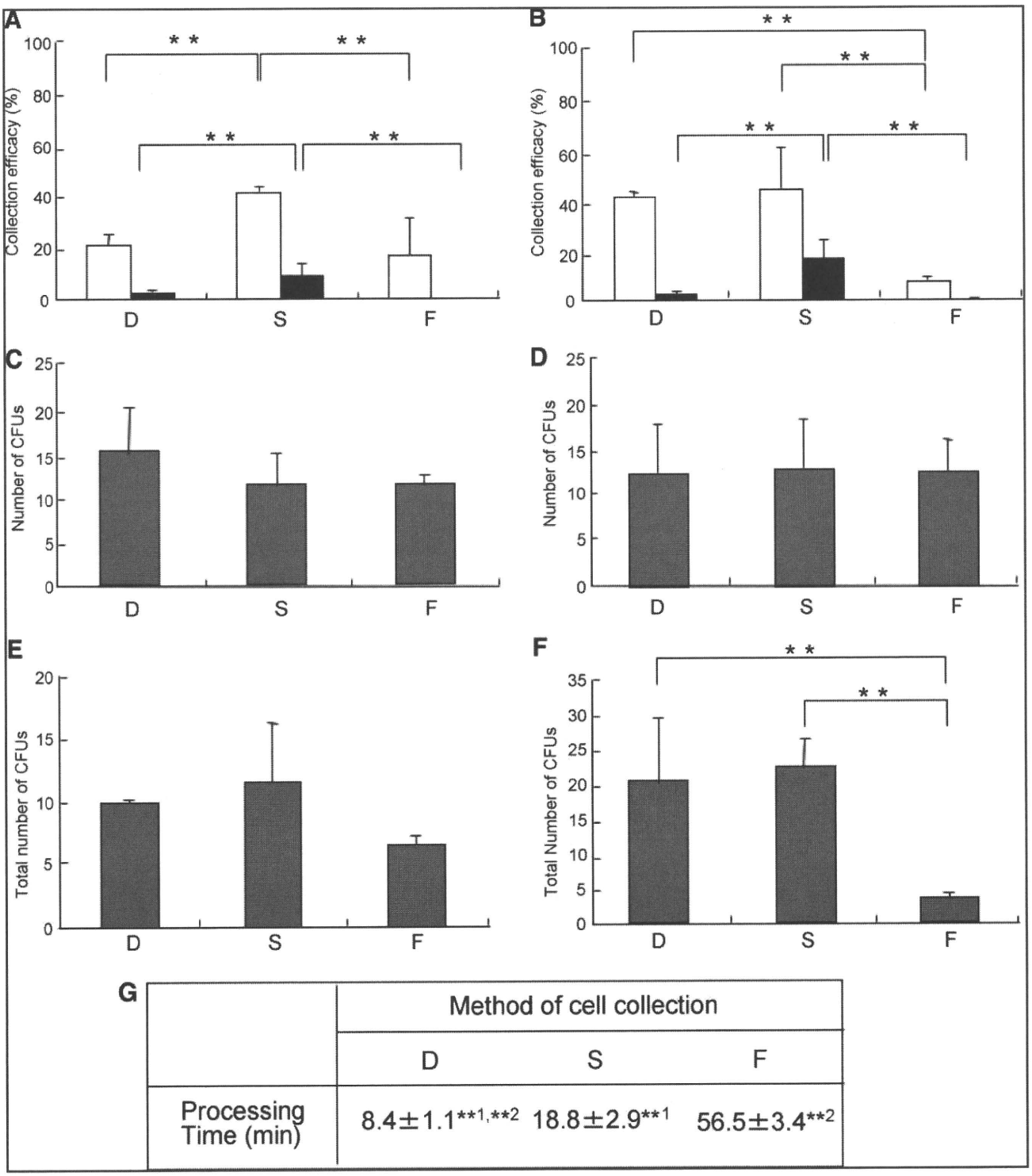

G

	Method of cell collection		
	D	S	F
Processing Time (min)	8.4±1.1**1,**2	18.8±2.9**1	56.5±3.4**2

FIG. 3. Device selectively prepares MNCs with CFUs. Collection efficacy for MNCs (white box) and erythrocytes (black box) isolated with each method from canine (**A**) and human (**B**) bone marrow. D, S, or F indicates each method described in Materials and Methods section. $^{**}p < 0.01$. Number of CFUs derived from equal numbers (2.5×10^5) of MNCs isolated by each method from canine (**C**) and human (**D**) bone marrow. Total number of CFUs derived from equal amounts of canine (**E**) and human (**F**) bone marrow using each method. $^{**}p < 0.01$. (**G**) Processing time for each method. $^{**1}p < 0.01$; $^{**2}p < 0.01$.

Selective collection of colony-forming cells from bone marrow by the device

Next, the selectivity of the device was analyzed using cells derived from canine (Fig. 2E, F) and human (Fig. 2G, H) bone marrow. In both cases, most erythrocytes passed through the filter and were collected in the flow-through fraction. Only a few were found in the collected fraction (data not shown). For canine bone marrow, the number of MNCs was significantly smaller in the collected fraction than in the

flow-through fraction ($p = 0.002$; Fig. 2E). The number of CFUs, however, was much higher in the collected fraction ($p < 0.001$; Fig. 2F). For human bone marrow, the number of MNCs in the collected and flow-through fraction did not differ (Fig. 2G). However, the number of CFUs was much higher in the collected fraction than in the flow-through fraction ($p < 0.001$; Fig. 2H). These results indicated the selective collection of CFUs by the device.

Comparison of method D with methods S and F

The biological properties of cells isolated by each of the three methods were compared. First, we compared the collection efficacy of method D with that of method S or F. ANOVA revealed significant differences among the collection efficacies for MNCs (canine, $p = 0.024$; human, $p = 0.0002$). Comparisons between individual methods were then carried out using Turkey's *post hoc* test. For canine bone marrow, the collection efficacy for MNCs was significantly lower with method D ($20.7 \pm 4.2\%$) than method S ($41.6 \pm 1.6\%$) ($p < 0.01$; Fig. 3A), and the same between method D and method F ($16.8 \pm 14.0\%$) (Fig. 3A). As for contamination by erythrocytes, method S showed larger numbers than method D or F. For human bone marrow, there was no difference in collection efficacy between method D ($40.5 \pm 14.5\%$) and method S ($43.9 \pm 10.8\%$) (Fig. 3B), and method F ($7.3 \pm 1.8\%$) was significantly less efficient than method D ($p < 0.01$; Fig. 3B). The number of contaminating RBCs was again high with method S (Fig. 3B). Next, the MNCs collected by each method were seeded on plastic dishes, and the number of CFUs was counted 14 days later. ANOVA indicated no significant difference among the numbers of CFUs of MNCs prepared by the three methods in canine ($p = 0.40$) and human bone marrow ($p = 0.95$) (Fig. 3C, D). From the results on collection efficacy and number of CFUs, the total number of CFUs isolated from bone marrow was calculated for each method. In the case of canine bone marrow, the total number of CFUs with method D (10.1 ± 0.2) was equivalent to that with method S (11.7 ± 4.7) and much larger than that with method F, but not significant (6.6 ± 0.1) (Fig. 3E). Similar results were obtained with human bone marrow cells. The total number of CFUs with method D (20.3 ± 9.4) was equivalent to that with method S (22.3 ± 4.4), and much larger than that with method F (3.6 ± 1.0) ($p < 0.01$; Fig. 3F). These results indicated that the device collected colony-forming cells from bone marrow with an efficacy equal to that of current methods requiring centrifugation. In addition, the processing time for method D (8.4 ± 1.1 min; Fig. 3G) was significantly shorter than that for the other methods (method S, 18.8 ± 2.9 min; method F, 56.5 ± 3.4 min) (ANOVA, $p < 0.001$; Turkey's *post hoc* test, $p < 0.01$; Fig. 3G).

Expression of MSC markers in isolated BMSCs

To compare the cell population isolated by each of the three methods, the expression of cell surface markers was analyzed by fluorescence-activated cell sorting (FACS). Because a combination of markers is more reliable, we focused on $CD10^+/CD271^+$, $CD90^+/CD271^+$, or $CD106^+/STRO\text{-}1^+$ double-positive cells. The $CD90^+/CD271^+$ and the $CD106^+/STRO\text{-}1^+$ populations were significantly larger among cells collected by method D than those collected by method S or method F (ANOVA, $p < 0.001$; Turkey's *post hoc* test, $p < 0.01$ for $CD90^+/CD271^+$, $p < 0.05$ for $CD106^+/STRO\text{-}1^+$, respectively; Fig. 4A, B).

Differentiation potential of isolated BMSCs

To analyze their potential to differentiate, the BMSCs isolated by each of the methods were propagated on culture

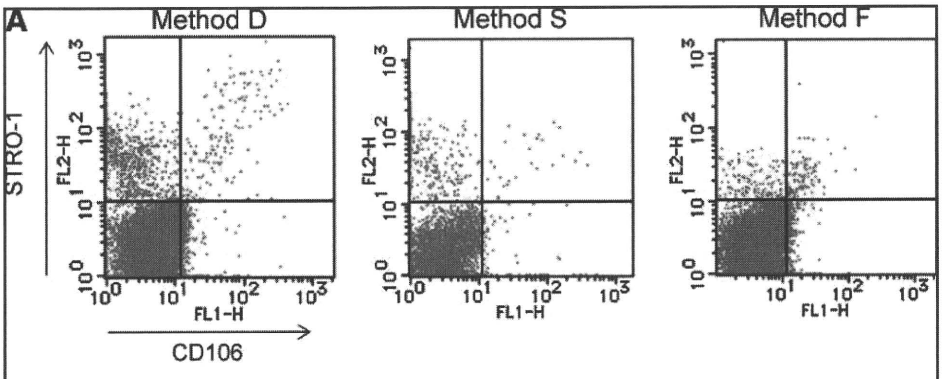

B

Markers	Fraction of double positive cells: Method D	Method S	Method F
$CD10^+$ / $CD271^+$	0.16 ± 0.05	0.13 ± 0.05	0.13 ± 0.02
$CD90^+$ / $CD271^+$	0.13 ± 0 **1**2	0.06 ± 0.01 **1*3	0.01 ± 0.01 **2*3
$CD90^+$ / $CD166^+$	0.31 ± 0.02	0.18 ± 0.12	0.23 ± 0.15
$CD106^+$ / $STRO\text{-}1^+$	1.61 ± 0.37 *1*2	0.48 ± 0.19 *1	0.71 ± 0.42 *2

FIG. 4. Device selectively prepares MNCs, which express mesenchymal marker. (**A**) FACS analysis of CD106 and STRO-1 on MNCs isolated by each method. (**B**) Fraction of cells double-positive for mesenchymal stem cell (MSC) markers among MNCs isolated by each method. **1,**2$p < 0.01$; *1,*2,*3$p < 0.05$.

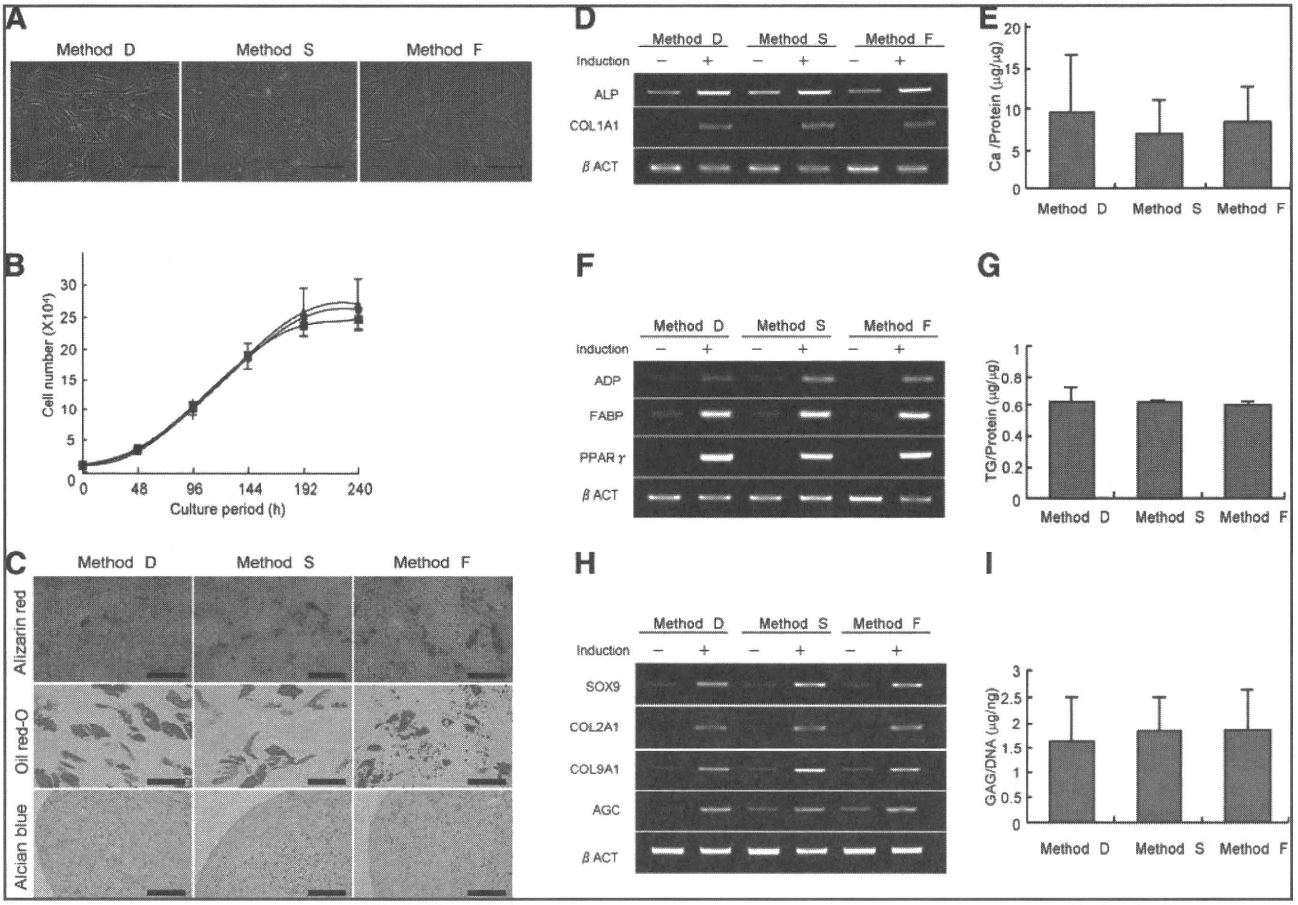

FIG. 5. Growth and differentiation potential of human BMSCs isolated by each method. The same numbers of BMSCs isolated by the three methods from human bone marrow were propagated on culture dishes for 2 weeks under standard conditions. (**A**) Microscopic views of cultured BMSCs isolated by each method. Magnification, 100×. Scale bars = 100 μm. (**B**) Growth of cultured BMSCs isolated by each method. ●, Method D; ▲, method S; ■, method F. (**C**) Differentiation potential of BMSCs isolated by each method. Osteogenic differentiation was analyzed by alizarin red staining. Magnification, 100×. Scale bars = 100 μm. Adipogenic differentiation was analyzed by oil red-O staining. Magnification, 100×. Scale bars = 100 μm. Chondrogenic differentiation was analyzed by alcian blue staining. Magnification, 40×. Scale bars = 300 μm. (**D**) Expression of bone-related genes before and after osteogenic induction. *ALP*, alkaline phosphatase. (**E**) Ca content after osteogenic induction. Ca, calcium. (**F**) Expression of fat-related genes before and after adipogenic induction. *ADP*, adipsin; *FABP*, fatty acid–binding protein; *PPARγ*, peroxisome proliferator-activated receptor gamma. (**G**) TG content after adipogenic induction. TG, triglyceride. (**H**) Expression of cartilage-related genes before and after chondrogenic induction. *AGC*, aggrecan. (**I**) GAG content after chondrogenic induction. GAG, glycosaminoglycan.

dishes and incubated for 2 weeks under standard growth conditions for MSCs. They were then induced to undergo osteogenesis, adipogenesis, and chondrogenesis. The morphology of the cells isolated by each of the methods was almost the same for both canine (Supplemental Fig. S2A, available online at www.liebertonline.com) and human (Fig. 5A) BMSCs. There was no difference in growth profile among the three methods in canine (Supplemental Fig. S2B, available online at www.liebertonline.com) or human (Fig. 5B) BMSCs. Osteogenic differentiation potential was evaluated with histochemical (alizarin red staining; Fig. 5C), mRNA expression (expression of the *ALP* and *COL1A1* genes; Fig. 5D), and biochemical (calcium content; Fig. 5E) analyses. There was no significant difference among the cells isolated by each of the three methods (ANOVA, $p = 0.61$). Similar results were observed in adipogenic differentiation

FIG. 6. Regeneration of bone tissues by cells isolated with the device. Data for six dogs at 4 weeks after the operation are presented. Frontal (**A**) and sagittal (**B**) views of micro-computed tomography. (**C**) Morphometrical analyses. The results of X-ray and micro-computed tomography were evaluated using the criteria described in the Materials and Methods section. Bone weight and volume were actually measured. $^{**}p < 0.01$; $^{*}p < 0.05$. CHR, carpal height ratio. (**D**) Histological analyses by hematoxylin–eosin staining. Magnification, 100×. Scale bar = 500 μm. (**E**) Fraction of regenerated bone tissue of each grade. Grade 1, white box; grade 2, gray box; grade 3, black box. $^{*}p < 0.05$. (**F**) Histological analyses using silver impregnation staining. Magnification, 200×. Scale bar = 200 μm. (**G**) Fraction of β-tricalcium phosphate with integrated collagen fibers of each grade. Grade 1, white box; grade 2, gray box; grade 3, black box. $^{*}p < 0.05$.

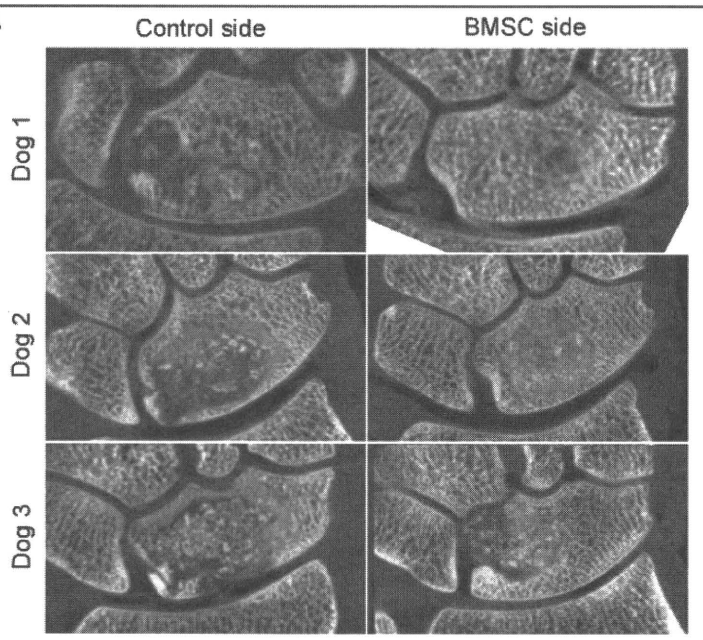

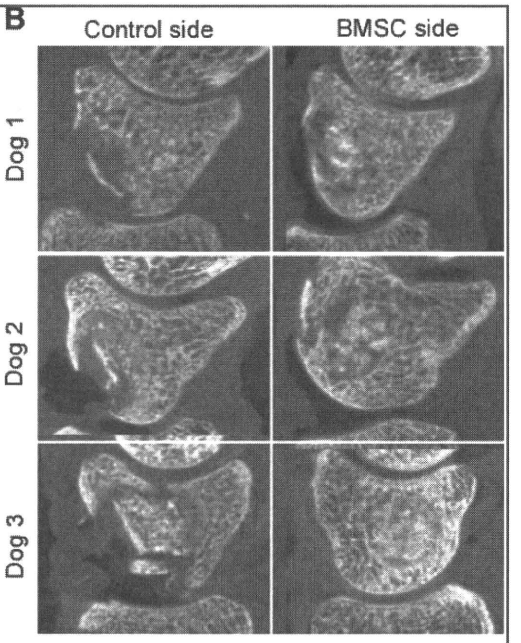

C

	X-ray evaluation		Micro CT evaluation			Actual Measurement		
	CHR	Ståhl index (%)	Bone Volume (cm^3)	Total Volume (cm^3)	Bone ratio	Weight (g)	Volume (cm^3)	Weight/Volume
Control side	0.30 ±0.03 * *	67.6 ±2.4 *	0.56 ±0.07 * *	0.81 ±0.11	0.67 ±0.03 * *	1.78 ±0.22 *	1.33 ±0.16 *	1.34 ±0.03 *
BMSC side	0.32 ±0.03 * *	72.1 ±6.3 *	0.64 ±0.06 * *	0.85 ±0.10	0.76 ±0.03 * *	1.83 ±0.19 *	1.34 ±0.15 *	1.38 ±0.04 *

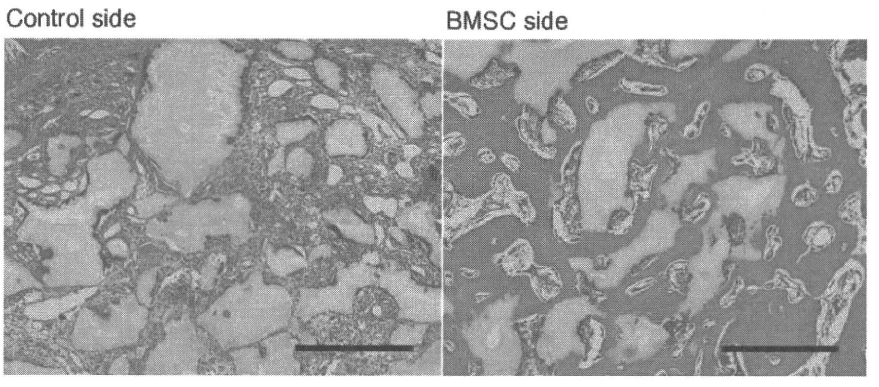

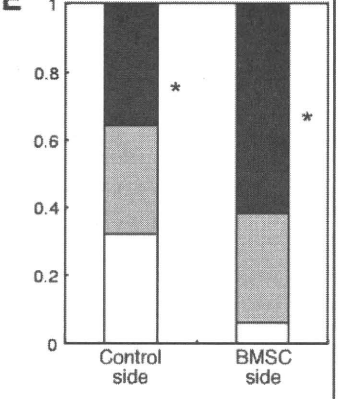

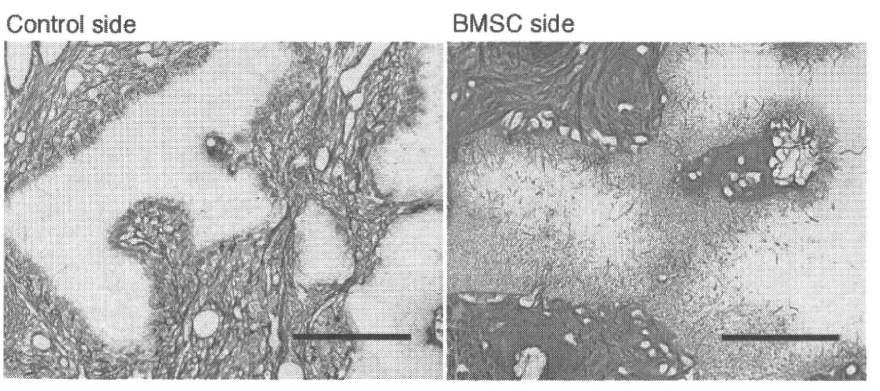

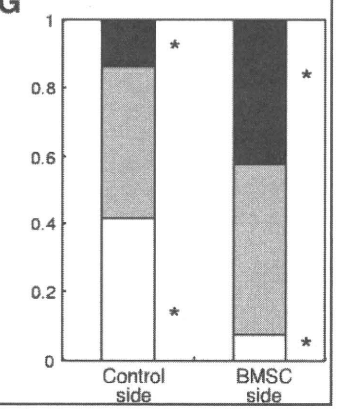

(ANOVA, $p = 0.41$; Fig. 5C, F, G) and chondrogenic differentiation (ANOVA, $p = 0.97$; Fig. 5C, H, I). Same results were obtained in the analyses of canine BMSCs (Supplemental Fig. S2C, available online at www.liebertonline.com). These results suggested that BMSCs isolated by each of the three methods had the multidirectional differentiation potential of MSCs.

Regeneration of bone tissues by cells isolated with the device

To confirm the *in vivo* osteogenic potential of cells collected with the device, we used the cells to regenerate bone tissues in a model of osteonecrosis using canine scapho-lunates, which we established previously.[15] Micro-CT findings at 4 weeks after the operation indicated bone regeneration to be more prominent on the BMSC side than control side in all cases (Fig. 6A, B). Carpal height ratio and the Ståhl index calculated from plain X-rays show the degree of collapse of scapholunate bone. Both parameters were significantly higher on the BMSC side than control side (Fig. 6C). Total volume and bone volume were analyzed from the micro-CT data. Bone volume and therefore bone ratio were greater on the BMSC side (Fig. 6C). Both actual weight and volume were also significantly higher on the BMSC side (Fig. 6C). These quantitative analyses suggested that the application of BMSCs prepared by the device contributed significantly to bone regeneration.

After the physical and radiological examinations, samples were processed for histological analyses. Microscopic findings of samples taken from the control side showed that a large amount of β-TCP remained unabsorbed, although multinucleated giant cells were found adjacent to β-TCP. In contrast, abundant new bone with the active absorption of β-TCP by multinucleated giant cells was found on the BMSC side (Fig. 6D). The extent to which β-TCP was absorbed as new bone formed was scored using criteria described in the Materials and Methods section. The grade 3 fraction was significantly larger on the BMSC side ($p = 0.032$; Fig. 6E).

To analyze the interaction between the prepared cells and β-TCP, silver impregnation staining was performed (Fig. 6F). The staining shows the invasion of collagen fibers into biodegradable materials. Collagen fibers in β-TCP granules adjacent to regenerated bone tissue were abundant on the BMSC side, but rare on the control side (Fig. 6F). Quantitative analyses showed the extent of the invasion to be significantly greater on the BMSC side ($p = 0.034$; Fig. 6G). These results suggested that BMSCs prepared using the device enhanced bone regeneration *in vivo*.

Discussion

Bone marrow cells consist of two types of MNCs: hematopoietic cells including hematopoietic stem cells, and stromal cells including MSCs. Approximately 99% of MNCs in bone marrow belong to the former population, and among the stromal cells, less than 5% have multidirectional differentiation potential compatible with the concept of MSCs. Therefore, the proportion of MSCs among bone marrow MNCs is estimated at less than 0.05%.[19] To obtain BMSCs including MSCs from bone marrow, it is essential to separate the hematopoietic MNCs.

Takenaka developed a novel filter composed of nonwoven fabrics to trap peripheral leukocytes for the treatment of autoimmune disease.[10] Because erythrocytes are deformed, which allows them to pass through small pores and have low adhesiveness, they can be separated from MNCs by the filter.[10] They used fibers 1.7 μm in diameter, because all the leukocytes were trapped when the fiber was less than 3 μm in diameter.[10] This filter, however, is not applicable to the separation of MSCs from hematopoietic MNCs, both of which will be captured, making it difficult to separate them by cell size. Therefore, we used fibers 15 μm in diameter with greater affinity for BMSCs than hematopoietic MNCs. MSCs are more adherent than hematopoietic cells.[4,19] MSCs adhere much more tightly to highly hydrophilic and rough surfaces than to hydrophobic and smooth surfaces.[20] The contact angle of the nonwoven fabric in the current device is estimated to be 20°, which is highly hydrophilic and may make it possible to trap MSCs in the device. This adherent trapping method may prevent excess shearing stress caused by the flow. Cells isolated by the device showed no increase in bradykinine or lactate dehydrogenase (LDH) (data not shown). In addition, mRNA expression of the *p16* and *p53* genes was not increased, and the karyotype showed no abnormalities (data not shown).

In terms of its potential clinical applications, the device has several advantages. The filter is composed of rayon and polyethylene. Rayon is used for the dialysis membranes of hemodialyzers and known to decrease platelet activity.[21] Polyethylene is a biomaterial employed in total hip replacement and as a scaffold for tissue engineering.[22] Therefore, all the materials are safe for clinical use. The isolation of BMSCs in a closed system is a major advantage of this device. Centrifugation requires mixing with an appropriate solution, which has to be performed in an open system. Current guidelines require the centrifugation process to be performed in an isolated area with specialized equipment. Because all steps can be done in a closed system, the device can isolate BMSCs from bone marrow on the operation table. Further, processing time is shorter than for the other two methods (Fig. 3G), which may help to reduce cell death during the isolation procedures. In addition, the method does not require special skills, which will help to obtain constant results and also be an advantage for clinical application.

We have shown that in terms of differentiation potential, the cells isolated using the device were equivalent to those prepared by current methods using centrifugation. The total number of CFUs obtained from bone marrow was equal to that achieved with method S and higher than that obtained with method F, suggesting that the device recovers almost all cells with the ability to form CFUs. FACS analyses showed that the method was superior to others in terms of the recovery of the MSC marker-positive population. CD10, CD44, CD90, CD106, and STRO-1 are considered surface markers of MSCs,[13,23] and, recently, CD271 was identified as a marker of MSCs.[24] The fractions of $CD90^+/CD271^+$ cells were larger among cells collected using the device than those isolated with the other two methods (Fig. 4). The $CD106^+/STRO\text{-}1^+$ fraction ($1.61 \pm 0.37\%$; Fig. 4) was even larger than that collected by FACS ($1.4 \pm 0.3\%$),[25] which has a risk of microbial contamination and unfavorable effects. We have no clear explanation for this selective collection. Because $CD106^+/STRO\text{-}1^+$ cells attach to plastic dish efficiently and have high colony-forming activity,[26] one possibility is that $CD106^+/STRO\text{-}1^+$ cells have high affinity to the filter materials used in the device. Finally, we have shown that the direct application of the trapped cells without *ex vivo* cultivation assisted the regeneration of bone

tissue *in vivo* (Fig. 6), although the role of transplanted cells may not be simply to reconstitute bone tissues by themselves but also to produce cytokines stimulating host cells,[15] suggesting that BMSCs collected with the new device on the operating table could be used for conditions requiring an acceleration of bone regeneration such as the nonunion of bone fractures.

Acknowledgments

We thank Dr. H. Iwata for suggestions and Drs. M. Neo, S. Fujibayashi, M. Takemoto, H. Ito, and H. Yoshitomi for clinical samples. This work was supported by Grants-in-aid for Scientific Research from the Japan Society for the Promotion of Science; from the Ministry of Education, Culture, Sports, Science, and Technology; from the Ministry of Health, Labor, and Welfare; and from the New Energy and Industrial Technology Development Organization.

Disclosure Statement

No competing financial interests exist.

References

1. Caplan, A.I. Mesenchymal stem cells. J Orthop Res **9,** 641, 1991.
2. Wagner, W., and Ho, A.D. Mesenchymal stem cell preparations comparing apples and oranges. Stem Cell Rev **3,** 239, 2007.
3. Peterson, E.A., and Evans, W.H. Separation of bone marrow cells by sedimentation at unit gravity. Nature **214,** 824, 1967.
4. Caterson, E.J., Nesti, L.J., Danielson, K.G., and Tuan, R.S. Human marrow-derived mesenchymal progenitor cells: isolation, culture expansion, and analysis of differentiation. Mol Biotechnol **20,** 245, 2002.
5. Li, Y., Ma, T., Yang, S.T., and Kniss, D.A. Thermal compression and characterization of three-dimensional nonwoven PET matrices as tissue engineering scaffolds. Biomaterials **22,** 609, 2001.
6. Takahashi, Y., and Tabata, Y. Effect of the fiber diameter and porosity of non-woven PET fabrics on the osteogenic differentiation of mesenchymal stem cells. J Biomater Sci Polym Ed **15,** 41, 2004.
7. Ma, Z., Kotaki, M., Yong, T., He, W., and Ramakrishna, S. Surface engineering of electrospun polyethylene terephthalate (PET) nanofibers towards development of a new material for blood vessel engineering. Biomaterials **26,** 2527, 2005.
8. Gador, W., and Jankowska, E. Filtration properties of nonwovens. Int J Occup Saf Ergon **5,** 361, 1999.
9. Gorman, N.E. Nonwoven materiel: manufacturing processes for sterilization wraps. Hosp Mater Manage Q **9,** 1, 1988.
10. Takenaka, Y. Lymphocytapheresis. Artif Organs **20,** 914, 1996.
11. Onodera, H., Abe, Y., Yoshida, M., Yamawaki, N., Yamashita, Y., Matsuo, H., Ichinose, K., Otsuru, I., and Shibuya, N. A new device for selective removal of $CD4^+$ T cells. Ther Apher **2,** 37, 1998.
12. Shibata, K.R., Aoyama, T., Shima, Y., Kenichi, F., Otsuka, S., Furu, M., Kohne, Y., Ito, K., Fujibayashi, S., Meo, M., Nakayama, T., Nakamura, T., and Toguchida, J. Expression of the p16INK4A gene is associated closely with senescence of human mesenchymal stem cells and is potentially silenced by DNA methylation during *in vitro* expansion. Stem Cells **25,** 2371, 2007.
13. Pittenger, M.F., Mackay, A.M., Beck, S.C., Jaiswal, R.K., Douglas, R., Mosca, J.D., Moorman, M.A., Simonetti, D.W., Craig, S., and Marshak, D.R. Multilineage potential of adult human mesenchymal stem cells. Science **284,** 143, 1999.
14. Fukiage, K., Aoyama, T., Shibata, K.R., Otsuka, S., Furu, M., Kohno, Y., Ito, K., Jin, Y., Fujita, S., Fujibayashi, S., Neo, M., Nakayama, T., Nakamura, T., and Toguchida, J. Expression of vascular cell adhesion molecule-1 indicates the differentiation potential of human bone marrow stromal cells. Biochem Biophys Res Commun **365,** 406, 2008.
15. Ikeguchi, R., Kakinoki, R., Aoyama, T., Shibata, K.R., Otsuka, S., Fukiage, K., Nishijo, K., Ishibe, T., Shima, Y., Otsuki, B., Azuma, T., Tsutsumi, S., Nakayama, T., Otsuka, T., Nakamura, T., and Toguchida, J. Regeneration of osteonecrosis of canine scapholunate using bone marrow stromal cells: possible therapeutic approach for Kienböck disease. Cell Transplant **15,** 411, 2006.
16. Youm, Y., McMurthy, R.Y., Flatt, A.E., and Gillespie, T.E. Kinematics of the wrist. I. An experimental study of radial-ulnar deviation and flexion-extension. J Bone Joint Surg Am **60,** 423, 1978.
17. Goldfarb, C.A., Hsu, J., Gelberman, R.H., and Boyer, M.I. The Lichtman classification for Kienböck's disease: an assessment of reliability. J Hand Surg Am **28,** 74, 2003.
18. Ogose, A., Kondo, N., Umezu, H., Hotta, T., Kawashima, H., Tokunaga, K., Ito, T., Kudo, N., Hoshino, M., Gu, W., and Endo, N. Histological assessment in grafts of highly purified beta-tricalcium phosphate (OSferion) in human bones. Biomaterials **27,** 1542, 2006.
19. Chamberiain, G., Fox, J., Ashton, B., and Middleton, J. Concise review: mesenchymal stem cells: their phenotype, differentiation capacity, immunological features, and potential for homing. Stem Cells **25,** 2739, 2007.
20. Kim, M.S., Shin, Y.N., Cho, M.H., Kim, S.H., Kim, S.K., Cho, Y.H., Khang, G., Lee, I.W., and Lee, H.B. Adhesion behavior of human bone marrow stromal cells on differentially wettable polymer surfaces. Tissue Eng **13,** 2095, 2007.
21. Thijs, A., Grooteman, M.P., Zweegman, S., Nubé, M.J., Huijgens, P.C., and Stehouwer, C.D. Platelet activation during haemodialysis: comparison of cuprammonium rayon and polysulfone membranes. Blood Purif **25,** 389, 2007.
22. Tessmar, J.K., and Göpferich, A.M. Customized PEG-derived copolymers for tissue-engineering applications. Macromol Biosci **7,** 23, 2007.
23. Deans, R.J., and Moseley, A.B. Mesenchymal stem cells: biology and potential clinical uses. Exp Hematol **28,** 875, 2000.
24. Bühring, H.J., Battula, V.L., Treml, S., Schewe, B., Kanz, L., and Vogel, W. Novel markers for the prospective isolation of human MSC. Ann NY Acad Sci **1106,** 262, 2007.
25. Gronthos, S., and Zannettino, A.C. A method to isolate and purify human bone marrow stromal stem cells. Methods Mol Biol **449,** 45, 2008.
26. Gronthos, S., Zannettino, A.C., Hay, S.J., Shi, S., Graves, S.E., Kortesidis, A., and Simmons, P.J. Molecular and cellular characterisation of highly purified stromal stem cells derived from human bone marrow. J Cell Sci **116,** 1827, 2003.

Address correspondence to:
Tomoki Aoyama, M.D., Ph.D.
Institute for Frontier Medical Sciences
Kyoto University
53 Kawahara-cho
Shogoin, Sakyo-ku
Kyoto 606-8507
Japan

E-mail: blue@frontier.kyoto-u.ac.jp

Received: December 21, 2008
Accepted: April 13, 2009
Online Publication Date: July 6, 2009

This article has been cited by:

1. Helena Motaln, Cristian Schichor, Tamara T. Lah. 2010. Human mesenchymal stem cells and their use in cell-based therapies. *Cancer* **116**:11, 2519-2530. [CrossRef]

The International Journal of Transfusion Medicine
Vox Sanguinis

Vox Sanguinis (2010) **98**, 538–546

DOI: 10.1111/j.1423-0410.2009.01290.x

ORIGINAL PAPER

Risk-adjusted assessment of incidence and quantity of blood use in acute-care hospitals in Japan: an analysis using administrative data

M. Sekimoto,[1] Y. Imanaka,[1] T. Shirai,[1] H. Sasaki,[1] T. Komeno,[2] J. Lee,[1] K. Yoshihara,[1] E. Ashihara[3] & T. Maekawa[3]

[1]*Department of Healthcare Economics and Quality Management, Kyoto University School of Public Health, Kyoto, Japan*
[2]*Department of Hematology, National Hospital Mito Medical Center, Kyoto, Japan*
[3]*Department of Transfusion Medicine and Cell Therapy, Kyoto University Hospital, Kyoto, Japan*

Background and Objectives Continuous monitoring of blood use and feedback on transfusions are effective in decreasing inappropriate blood transfusions. However, traditional methods of monitoring have practical challenges, such as the limited availability of experts and funding. Administrative data including a patient classification system may be employed for risk-adjusted assessment of hospital-wide blood use.

Materials and Methods We conducted an audit of blood use at two hospitals and determined proportions of appropriate blood use at each hospital. We then used administrative data of 587 045 cases provided by 73 hospitals to develop two mathematical models to calculate risk-adjusted use of blood products. The first model is a logistic regression model to predict the percentage of transfused patients. Patient demographics, surgery and diagnostic groups were utilized as predictors of transfusion. The second model is a case-mix adjusted model which predicts hospital-wide use of units of blood products from the distribution of diagnosis-related groups. For each model, the observed to expected (O/E) ratio of blood use in each hospital was calculated. We compared resultant ratios with proportions of appropriate blood use in two of the hospitals studied.

Results Both models showed good prediction abilities. O/E ratios calculated using the two models were relevant to proportions of appropriate transfusions.

Conclusions Risk-adjusted assessments of blood product use based on administrative data allow hospital-wide evaluation of transfusion use. Comparing blood use between different hospitals contributes toward establishing appropriate transfusion practices.

Key words: administrative data, blood usage, diagnosis-related group, platelets, red cells

Received: 20 July 2009,
revised 8 November 2009,
accepted 8 November 2009,
published online 10 December 2009

Introduction

The value of blood transfusions to patients with haemorrhage, haematopoietic disorders and other critical illnesses is widely recognized. In recent years, transfusion medicine has faced many issues, including increases in transfusion-transmitted viral infections, as well as insufficient blood supply due to increasing demand for transfusions. From perspectives of patient safety, quality medical care and effective use of limited medical resources, it has become more important to use the minimum amount of blood necessary for each transfusion. Although guidelines have been developed by various organizations in different countries [1–6], adherence to guidelines is often poor. Previous research conducted in Japan and internationally has

Correspondence: Yuichi Imanaka, Department of Healthcare Economics and Quality Management, Kyoto University Graduate School of Medicine, Yoshida Konoe-cho, Sakyo-ku, Kyoto, 606-8501, Japan
E-mail: imanaka-y@umin.net

demonstrated great variation in physician and hospital use of blood products [7–11].

Several studies have shown that auditing and feedback on transfusions is effective in decreasing inappropriate blood transfusions [12]. The most widely used method is a retrospective review of medical records and blood orders conducted by experts to determine appropriateness of transfusions. Practical challenges because of the limited availability of experts and funding, however, have restricted these approaches to analysis of limited time periods and limited groups of patients.

Other studies have analysed blood usage using administrative healthcare databases (e.g., Medicare data). For these analyses, blood transfusion practices for several diagnostic groups and surgeries were described using the diagnosis-related group (DRG) classification [13–16]. Comparison of the frequency and amount of blood product use and blood transfusion policies for the same diagnostic groups at different medical institutions has made it possible to identify excessive blood product use at particular institutions. If we can predict blood product use from the distribution of DRGs by using administrative data and compare them to observed use, then we may be able to screen providers whose blood usage is above average.

In 2003, Japan introduced a new medical payment system based on Japan's unique patient classification system, called the 'diagnostic procedure combination (DPC)' like the Healthcare Resource Group (HRG) in the United Kingdom, the DPC payment system consists of unique diagnostic categories emphasizing clinical classification. Hospitals those utilize DPC for medical payment use a uniform format to produce discharge summary data (i.e., DPC data). In addition to patient demographics, disease category and type of surgery, DPC data includes detailed information about type and quantity of all blood products used for each patient.

In this study, we conducted a retrospective audit of blood use at two hospitals in Japan to examine underlying conditions for blood use and appropriateness of blood transfusion in each hospital. Also, by using DPC data provided by 73 acute-care hospitals in Japan, we developed multivariate regression models to predict hospital-wide use of red blood cell (RBC) transfusions and platelet transfusions. For the two models, we assessed risk-adjusted, hospital-wide use of RBC and platelet transfusions at the hospitals studied. Furthermore, we compared the risk-adjusted use of blood products with proportions of appropriate blood use at each hospital. If the prediction model can successfully detect providers or clinical areas where blood use is above-average, then we can screen for overuse of blood use targeting a large number of hospitals and populations. Such a method is promising as a potential tool that can replace traditional audits.

Materials and methods

Data source and study subjects

This study was approved by the Medical Ethics Committee of Kyoto University in Kyoto, Japan. The protocol was approved by the Institutional Review Board (IRB) of Kyoto University Graduate School of Medicine. Data were extracted from the Quality Indicator/Improvement Project (QIP). QIP collects DPC data from institutions and analyses healthcare processes, patient outcomes and disease management to provide feedback to participating hospitals. Hospitals in the QIP voluntarily join the project, and represent a variety of public, private, teaching and non-teaching hospitals with different case-mixes and specialties. A total of 75 hospitals participated in the project. Excluding two hospitals whose healthcare claim data were incomplete, a total of 73 hospitals were included in the analyses.

Diagnostic procedure combination data are created for each patient per hospitalization. The primary classifier in the record was the DPC code (one field), which is determined by the disease that consumed the largest amount of medical resources. The DPC code contains 14 digits; the first 10 digits represent the combination of disease category and surgical procedure; the last four digits represent comorbidities, complications, age of patients (in some diagnostic groups) and expensive treatment such as chemotherapy, artificial ventilation and central venous catheters. In addition to the hospital and patient identifier and the DPC code, data included items such as the final diagnosis (one field), primary diagnosis (one field), secondary diagnosis (one field), comorbidities and complications (nine fields) and surgery information (seven fields for each surgical procedure, involving ≤ 5 surgeries).

By combining medical claim data to clinical data, it was possible to know the specific conditions for use of transfusions and details on the type, amount and other information on blood products transfused. From the DPC database, we selected approximately 661 000 consecutive records of patients discharged from 73 hospitals in Japan between April 2006 and March 2008. These records were represented the sample analysed in this study. Approximately 74 300 cases, in which patients were under 20-years old, were excluded. A total of 587 045 cases were included in the analyses.

Analyses of blood transfusion practices and identification of risk factors

We conducted a retrospective audit of blood product use in two (Hospital A and Hospital B) of the 73 hospitals studied, and surveyed underlying conditions for which transfusions were performed. These two hospitals were among eight hospitals that have participated in QIP since its inception;

both have more than 700 beds, and are teaching hospitals. Targets of audits were consecutive patients who received RBC or platelet transfusions during hospitalization and were discharged from the hospitals between July 2006 and September 2006. These patients were identified from the database, as well as from lists of patients transfused at the hospitals. Five of the authors (M.S, Y.I, T.S, H.S and K.Y) participated in the chart review. Through reviews of medical records, reviewers identified conditions (clinical course, findings of physical examinations and laboratory tests) in which a blood product was used. From the information collected, we attempted to determine the appropriateness of blood product use. Appropriateness was judged based on the 'Guidelines for blood transfusions' developed by the ad-hoc group of the Japanese Ministry of Health, Labor, and Welfare [17]. The Japanese guidelines were developed based on international guidelines and other national guidelines [2,18–21], and its recommendations are substantially similar to those of other guidelines. We also checked the accuracy of administrative claim data on timing, amount and type of blood product used. Some patients (e.g., those with haematopoietic diseases or chronic anaemia) received more than one blood transfusion during their hospitalization. For these cases, we reviewed the first episode of transfusion and judged the appropriateness of the transfusion decision. Differences in judgment were discussed among reviewers and one external expert until a final agreement on appropriateness was reached. The authors fed back results of the audits to chiefs of transfusion committees of each hospital, and obtained their consent.

Through audits at the two hospitals, we identified diagnoses, surgical procedures and comorbidities underlying the use of RBC and platelet transfusions. Using the ICD-10 code and surgical procedure classification code from the Ministry of Health and Welfare in Japan, 2006), we surveyed the frequency of these risk factors in the database, as well as proportions of transfused patients among patients with each risk factor.

Logistic regression model to predict proportions of transfused patients at hospitals

Using DPC data of 587 045 cases provided by 73 acute-care hospitals, we developed a multiple logistic regression model to predict proportions of transfused patients at each hospital. In this model, the dependent variable, the occurrence of blood transfusion during hospitalization, was defined as a binary variable. Each case received at least one blood transfusion during hospitalization was classified as '1; Used'. Each case that did not receive any blood transfusions during hospitalization was classified as '0; Not used'. Independent variables included risk factors, which either were identified through chart reviews at the two hospitals or were reported in previous studies to be associated with the risk of transfusion [14–16,22]. Performance of the logistic regression model was assessed by calculating the area under the receiver operating characteristic (ROC) curve. The area under a ROC curve relating relative proportions of correctly and incorrectly classified predictions over a wide and continuous range of threshold levels can measure discrimination capacity of the prediction rule [23,24]. Using the regression model, we calculated expected proportions of patients transfused at each hospital. By comparing observed (O) and expected (E) values, we calculated O/E ratios.

Case-mix adjusted model to predict total units of blood products transfused from the distribution of diagnostic groups at hospitals

The second model utilized the distribution of diagnostic groups to predict the total units of RBCs or platelets transfused at each hospital. In this model, we calculated the mean units of blood products used per case for each diagnostic group (defined by the first 10 digits, representing disease code + surgical code), and used these mean values as expected values for RBC or platelet use in that diagnostic group. All cases in each group were used to calculate means. Mean units used per case in the ith group can be represented by $Q(i)$, the number of cases belonging to that group can be represented by $N(i)$, and the total number of diagnostic groups can be represented by W. Thus, the expected total units of blood product used in the hospital can be described by the following formula:

$$\sum_{i=1}^{W} \{Q(i) \times N(i)\}$$

From the distribution of diagnostic groups in each hospital, we estimated total units of RBCs or platelets used at the hospital. By comparing expected and observed values, we calculated O/E ratios for total units transfused at each hospital. Predictive ability of this model was assessed by the correlation coefficient, r^2. Moreover, we compared results of the retrospective audit with O/E ratios. To assess case-mix adjusted blood product use, expected total RBC or platelet use was compared with observed values to obtain observed to expected ratios (O/E ratios) at each hospital. We used SPSS (Version 11, SPSS Inc., Chicago, IL) for all statistical analyses.

Results

Risk factors of blood transfusion

Table 1 shows characteristics of the hospitals in Japan that were studied, as well as the frequency and amount of RBC

Table 1 Characteristics of 73 studied hospitals and the distribution of blood products use in each hospital

Factor	Range	Percentile		
		25%	50%	75%
No. of bed	43–1106	239	350	530
No. of hospitalization (month)	93–2468	361	559	953
Mean length of stay (days)	9·6–41·0	13·2	15·2	18·2
Hospital mortality rate (%)	0·1–8·8%	3·4	4·5	5·2
No. of patients with RBC transfusion (100 beds/month)	0·8–22·6	5·2	7·5	10·1
No. of patients with PLT transfusion (100 beds/month)	0–6·1	0·65	1·2	2·4
All RBC units transfused (Units/100 beds/month)	2·7–228·6	33·3	50·2	73·7
All PLT units transfused (Units/100 beds/month)	0–499·3	19·1	45·7	120·0

RBC, red blood cell; PLT, platelet.

products and concentrated platelets transfused at the hospitals. Of the 587 045 cases targeted, 33 155 (5·7%) patients received RBC transfusions, and 7065 (1·2%) patients received platelet transfusions. Frequency of blood transfusion and number of units transfused per patient-bed varied greatly between hospitals. Based on retrospective audits at two hospitals (Hospitals A and B), Table 2 summarizes underlying conditions for use of RBC and platelet transfusions, as well as appropriateness of blood transfusions at each hospital.

From the retrospective audit, we identified patient characteristics, diagnoses and surgical procedures potentially associated with risk of blood transfusion. Table 3 shows the distribution of these potential risk factors in 587 045 cases in the database, as well as the probability of receiving ≥ 1 transfusion during hospitalization of the population with each risk factor. Cases with the risk were identified using the disease classification (ICD-10) code and surgery classification code (from the fee schedule system for medical reimbursement by the Ministry of Health and Welfare, Japan). Factors with the greatest risk for RBC transfusion included cardiovascular surgeries, haematopoietic malignancies, aplastic anaemia and myelodysplastic syndrome (MDS). Factors with the greatest risk for platelet transfusion included blood diseases such as acute leukaemia, aplastic anaemia and MDS, as well as cardiovascular surgery.

Logistic regression models predicting proportions of patients with transfusions

Table 4 shows risk factors for RBC and platelet transfusions and coefficients and odds ratios (ORs: 95% confidence intervals) of multiple logistic regression analyses. Greatest

Table 2 Underlying conditions of transfusion and proportions of appropriate transfusion

Underlying condition	Hospital A			Hospital B		
	n	(%)	Appropriate transfusion (%)	*n*	(%)	Appropriate transfusion (%)
RBC transfusion						
Acute bleeding	52	20	83	43	16	77
Perioperative						
Cardiovascular surgery	39	15	62	35	13	71
Others	55	21	55	50	19	66
Chronic anaemia						
Haematopoietic malignancies/ disorders	35	14	74	67	25	90
Others	52	20	77	47	18	89
Chronic bleeding	24	9	96	24	9	96
All	257	100	72	266	100	81
Platelet transfusion						
Haematopoietic malignancies/ disorders	30	38	13	51	59	78
Cancer	11	14	82	8	9	50
Surgery						
Cardiovascular surgery	23	29	17	12	14	83
Others	5	6	60	4	5	0
Others	10	13	30	12	14	17
All	79	100	29	87	100	64

GI indicates gastrointestinal; MDS. Myelodysplastic syndrome; RBC, red blood cell.